Landmarks in Earth Reinforcement, - Ochiai et al (eds),
© 2003 Swets & Zeitlinger, Lisse, ISBN 90 265 1863 3

Actual status of the application of the soil nailing to expressway cut-slope construction in Japan

M. Hirano
Japan Highway Services, Tokyo, Japan

ABSTRACT: It has been about twenty years since the soil nailing, a method that had been developed for reinforcing soil, was first used in expressway construction in Japan. Since then, this method has been subjected to laboratory tests, field tests and experimental work. In 1998 the Japan Highway Public Corporation established the application standard of the method on the basis of the results of these studies, in "Designing and Construction Procedure for the Soil Nailing Method". This paper discusses the actual status of the application of the method, focusing upon the safety management of the cut slope, results of long-term stability investigation and the essential points of the said Procedure, as well as the recent studies.

1 INTRODUCTION

The section between Ritto and Amagasaki of the Meishin Expressway (71 km), the first expressway in Japan, was opened in 1963, thirty-eight years ago. The total length planned for the expressway is 11,520 km. As of the end of March 2001, the expressway length totaled 6,861 km. Because of the topographical conditions of Japan, most expressways pass through mountainous districts. Consequently, the soil nailing method has been widely used for preventing collapse of cut slopes. The Yagiyama bypass (in Kyushu) project in 1982 was the first case in expressway constructions, where the soil nailing method was aggressively employed as a new concept of soil reinforcement. At about this time, laboratory tests[1),2),3)], field tests[4),5),6)], and test construction[7)] began. On the basis of the results of these tests, the Japan Highway Public Corporation (hereinafter referred to as JH) prepared guidelines[8)] and other documentation for the method. This led rapidly to increased use of the method in recent years. The investigation in 1999 showed that, in expressway construction projects, on a yearly basis, there were 74 sites about 100,000 m long in total, including both temporary and permanent works. The soil nailing method will find more extensive use along with construction of the second Tomei and Meishin Expressways and transversal expressways.

The Japanese Geotechnical Society established the Research Committee of Reinforced Slope Method (April 1993 to March 1996), which issued a report[9)] in March 1996. This report pointed out problems and goals for the reinforced slope method. These included setting the strength constant for the ground, evaluation of the effect of slope reinforcing works, evaluation of effects of slope protection, process of implementation using information technology, seismic performance and its evaluation method, durability of the permanent slope, landscaping, and development of new techniques. For achieving these goals, various institutes are actively engaged in research. This paper discusses the safety management of excavated slopes JH has conducted in cut earth reinforcing sites, results of investigation on the long-term safety, and the essential points of "Designing and Construction Procedure for Soil Nailing Method" established in 1998 [10)]. Recent research by the author is also presented here.

2 ACTUAL STATUS OF APPLICATION

Figure 1 shows the status of soil nailing works in expressway projects in 1999. The total length of the works is about 100,000 m. The cases where the soil nailing method was applied to steep slope excavation with an inclination 1 : 0.5 (63 degrees) or more account for about 40%. In steep mountainous districts, where the Second Tomei and Meishin Expressways and transversal expressways are being constructed, new specifications for the big-scale road projects including larger piers and abutments on slopes are required. Therefore, the steep slope is excavated with soil nailing, aiming to alleviate environmental impact, decrease excavated soil, and reduce work cost.

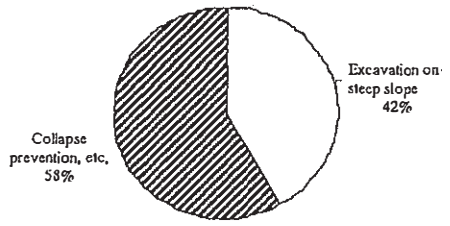

Figure 1. Application of reinforced slope method.

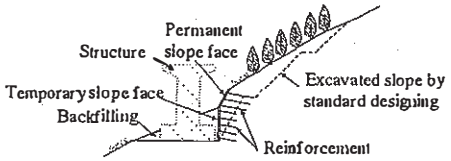

Figure 2. Excavation on steep slope.

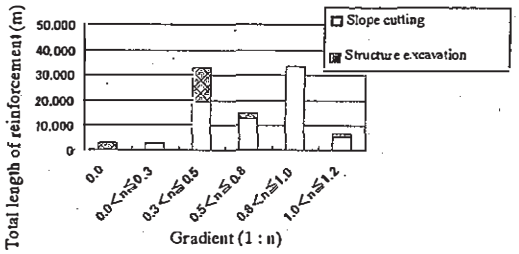

Figure 3. Total length of reinforcement and excavation slope.

Figure 3 illustrates the relationship between total length of the reinforcement and the slope gradient. In the case of structure excavation, the gradient often exceeds 1 : 0.5. This is because many bridges are constructed in steep mountainous sites.

In the case of the cut slopes for roads, gradients greater than 1 : 0.5 are also used as an alternative of block masonry at the lowest portion of slopes.

Figure 4 depicts the relationship between average reinforcement length and gradient. The average reinforcement length for vertical excavation may be up to about 6 m, while it is about 3 to 4 m regardless of the gradient, except for the range of $1.0 < n \leq 1.2$. The greater length of reinforcement in this range may be due to the fact that the length is determined by collapsing factors.

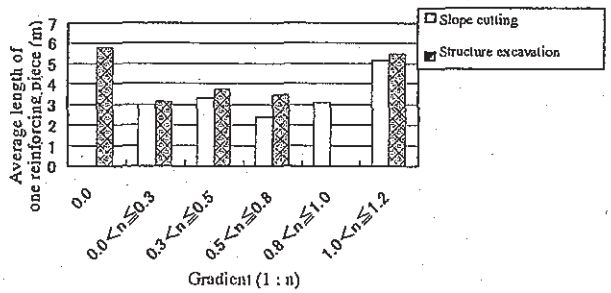

Figure 4. Average length of one reinforcing piece and excavation gradient.

3 PREVIOUS STUDIES

Out of the results of the studies by JH on the soil nailing method, we will discuss below the safety management of excavated surfaces and results of investigation on the long-term stability.

3.1 Safety management of excavated surface

Since the soil nailing method allows deformations, strict management of displacement is essential when an important structure exists over the excavated slope. The measurements in actual projects and full-scale experiments will be presented below, which were carried out to achieve satisfactory safety management of excavated slopes.

(1) Measurements in actual projects where steep slopes were excavated using the soil nailing method.

Table 1 shows the properties and specifications of the six experimental work sites. The geology of the sites ranged from relatively hard igneous rock to talus cone and fault fractured zone.

Figure 5 illustrates the distribution of ground displacement determined by borehole inclinometers at experimental work site A. In most points, soil displaces in such a way that it falls down toward the excavated surface. Along with the progress of excavation, the displacement increases.

Table 2 shows the displacements at the slope top and normalized horizontal displacement at the slope top δ_h/H (H = excavation height). In every site, the displacement at the slope top is small. Even at Site A where the normalized horizontal displacement at the slope top δ_h/H is at the maximum, it is only about 0.14%. This is a small magnitude within the range specified by the French standard[11] from 0.1 to 0.4%.

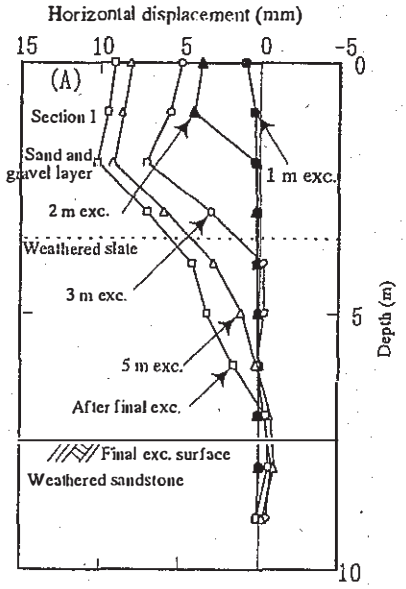

Figure 5. Distribution of ground displacement (A).

Table1. Overview of the experimental work sites

Site	Geology	Excavation height (m)	Excavation gradient	Reinforcement			Slope protection
				Diameter	Length (m)	Spacing (m)	
A	Sand and gravel, weathered slate	3.5	1:0.3	φ32	5.0	1.0×1.0	Shotcrete t=10cm
		3.5 Total 7.0	1:0.0		5.0	1.0×1.0	
B	Talus cone, weathered sandstone	2.0	1:0.5	D22	4.0	1.2×1.2	Shotcrete t=10cm +Spraying frame
		1.1	1:0.5	D22	4.0	1.2×1.2	
		9.9 Total 13.0	1:0.2	D19	3.0	1.5×1.5	Shotcrete t=5cm
C	Talus cone, sandstone, conglomerate	8.0	1:0.5	D25	4.0	1.0×1.0	Shotcrete t=10cm
D	Welded tuff	9.3	1:0.5	D19	2.0	1.5×1.5	Shotcrete t=15cm
		7.3 Total 16.3	1:0.0				Shotcrete t=5cm
E	Talus cone, granodiorite porphyry	5.8	1:0.3	D25	4.5	1.2×1.2	Shotcrete t=15cm
		2.67	1:0.3		2.0	1.5×1.5	
		4.0 Total 12.47	1:0.0		2.0	1.5×1.5	Shotcrete t=10cm
F	Weathered schist, fractured zone	12.8	1:0.5	φ32	6.0	1.2×1.2	Shotcrete t=5cm +Spraying frame

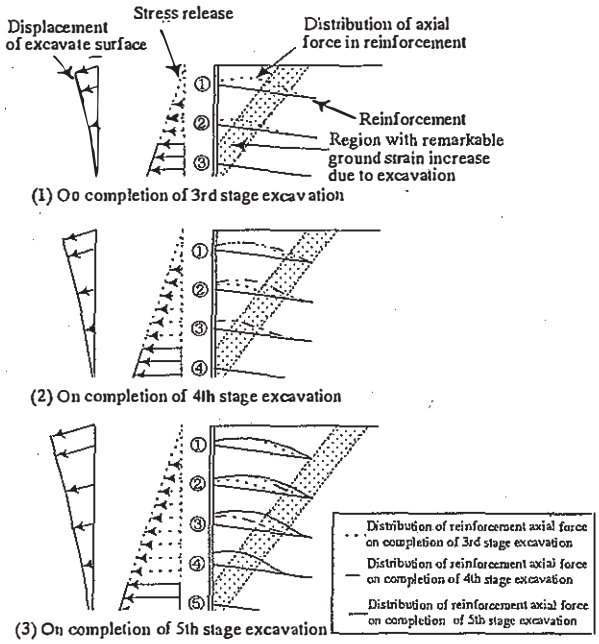

Figure 6. Schematic movement of cut slope.

Table 2. Displacement of slope top and normalized horizontal displacement.

Experimental work site	Slope top displacement		Normalized horizontal displacement
	Horizontal δ_h(cm)	Vertical δ_v(cm)	δ_h/H(%)
A	0.958	—	0.137
B	0.260	—	0.020
C	0.251	0.0	0.031
D	0.600	1.2	0.036
E	0.458	0.4	0.037
F	0.050	0.1	0.004

The behavior of nailed soil determined from the field measurements is summarized as depicted in Figure 6. The excavated surface tends to displace in such a manner that it falls down in the forward direction, when the reinforced slope is in the stable condition. Till the 3rd to 4th stage excavation, the maximum axial force in the reinforcement increases, and its position gradually moves toward the ground side. In the excavation after these stages, there is no significant change. This can be explained as follows. Till the 3rd to 4th stage excavation, strains are generated due to excavation in the ground between the excavated surface and reinforcement end, resulting in increased axial force in the reinforcement. But in the succeeding excavation, the region where ground strains occur moves beyond the reinforcement toward deeper side, and consequently there is no increase in axial force. Even in the excavation after the 3rd to 4th stages, the horizontal displacement at the slope top increases. This demonstrates that strains develop in the ground deeper than the reinforcement.

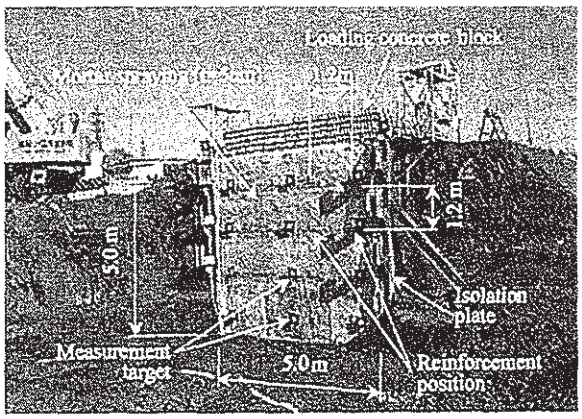

Figure 7. View of the full-scale test.

(2) Fracture behavior in the full-scale experiment [12]

To study the deformation behavior in fractures, a sandy embankment simulating a uniform natural slope was made as shown in Figure 7, and the loading test and excavation test were carried out using the soil nailing method. The banking material was sandy soil with gravel, N value of which after compaction was about 10. It is equivalent to that of talus cone deposit on a natural slope. In the experiment, as in the actual construction site, the cut slope was reinforced from top to bottom, layer by layer ("layer-by-layer placement"). Loading was conducted, by the use of polymer fiber (2 m x 1.2 m) and concrete blocks (0.2 m x 0.3 m x 0.15 m), They are flexible enough to follow the embankment deformation and can avoid fixation of the slip face till the final fracture. The test cases are summarized in Table 3.

Figure 8 depicts the displacements of the excavated surface just before the fracture. In the case without reinforcement, the excavated surface slipped downwards almost in parallel. In reinforced Case 2, the middle part of the excavated surface heaved when loaded. Furthermore, just before fracture, a larger horizontal excavated surface displacement occurred in the lower portion, while larger vertical displacement took place in the upper portion. This displacement behavior corresponds to the fracture mode with circular slip. From these facts, we know that, while the falling-forward deformation occurs during excavation, the ground stability is maintained, but on the verge of fracture, the middle and lower portions heave and the deformation mode changes from the falling-forward movement to the circular slip.

Table 3. Overview of the experimental cases.

Case	Non-reinforced case	Reinforced case 1	Reinforced case 2	Reinforced case 3
Slope gradient	1:0.3	1:00	1:00	1:0.1
Grout diameter	—	60	60	60
Material	—	Deformed bar SD345,D25	Deformed bar SD345,D25	Deformed bar SD345,D25
Reinforcement length	—	2.0m	2.5m	1.5m

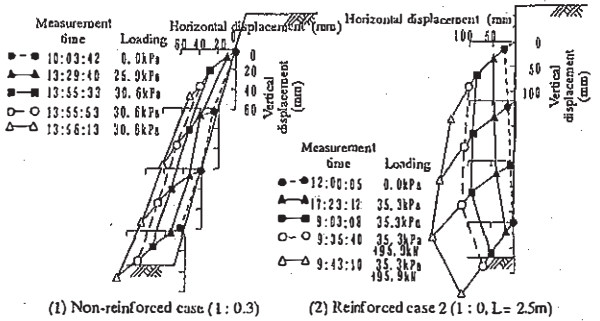

Figure 8. Displacement of excavated surface just before fracture.

The graphs in Figure 9 show the safety factor F_s given by the ultimate equilibrium equation plotted against the normalized horizontal displacement of slope top δ_h/H from excavation till fracture due to loading. This factor F_s does not include the safety factor (partial factor) of skin friction between grout and ground. The value of δ_h/H tends to increase abruptly when the safety factor F_s becomes 1.5 or less. In the reinforced cases, the limit of slope top normalized horizontal displacement stays generally within the range from 0.4 to 0.9%. In the non-reinforced case, the fracture occurred with a strain smaller than the reinforced cases, that is, with δ_h/H being less than 0.2%. The limit of slope top normalized horizontal displacement just before the fracture in the reinforced cases is larger than that of the non-reinforced case. This confirms that the earth reinforcement of the method presented here provides increased durability to the ground. When a steep slope is excavated using the soil nailing method, in a soil ground such as this test embankment, the excavated surface stability is maintained if $\delta h/H$ is not more than 0.4%.

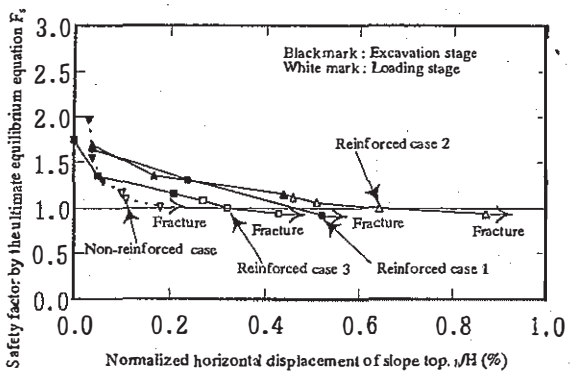

Figure 9. Variation of safety factor by the ultimate equilibrium equation vs. normalized horizontal displacement of slope top.

(3) Estimation of deformation magnitude of excavated slopes in bedrock

The full-scale test discussed above supposes soil slopes, so it is not directly applicable to soft rock or hard rock slopes. Through analysis of experiments by JH and cases implemented by other organizations, the allowable displacements of soft rock and hard rock slopes were estimated.

Figure 10 shows the relationship between excavation height H and slope top horizontal displacement δ_h, obtained from 47 cases including JH's experimental works, previous studies[13),14),15),16)], and questionnaire investigation. The slope top horizontal displacements of soft and hard rocks are smaller compared with soil ground.

Figure 11 illustrates the relationship between δ_h/H and modulus of deformation E_b of the borehole load test. In this figure, a limit line is also given, which was drawn referring to the inclination of the relationship between limit strain ε and elastic

modulus E_{50} determined by Sakurai through unconfined compressive strength tests[17]. In general, the larger the ground deformation coefficient, the smaller is the magnitude of δ_h/H.

Hence, safety of excavation is ensured, if the slope top normalized horizontal displacement is within the range not more than 0.3% for soft rock, and not more than 0.2 % for hard rock.

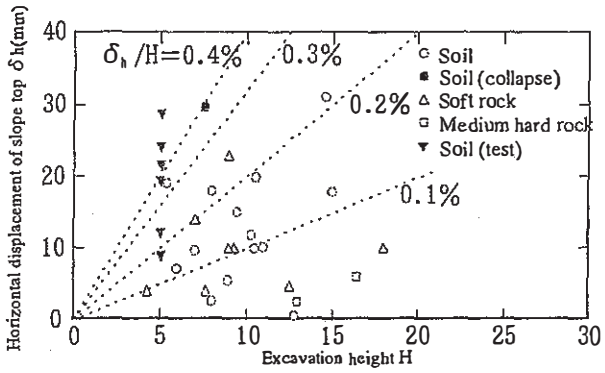

Figure 10. Horizontal displacement of slope top vs. excavation height.

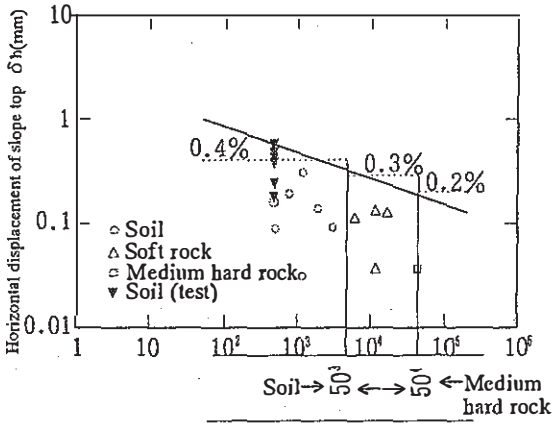

Figure 11. Horizontal displacement of slope top $\delta h/H$ vs. modulus of deformation Eb.

(4) Strain rate

In reinforced Case 1 of the full-scale test, fractures occurred during construction work, because the bondage between reinforcing bars and grout was broken due to insufficient strength of the grout. Referring to this case, the author studied the strain rate that is one of indexes for predicting fracture. The graphs in Figure 12 show the relationship between displacement/strain rate and elapsed time for the case where a fracture occurs in the course of construction, and the case of stable excavation respectively. In the case of stable excavation, after the displacement converged, the next stage was excavated. In contrast, fractures occurred when excavation was performed while the displacement did not converge. This resulted in abruptly increased strain, and led to fracture. We can conclude from this that when the next stage is excavated, even if the slope top normalized horizontal displacement develops at a very small pace, the slope is prone to fracture. In actual construction sites, it is vital to carefully monitor the convergence of displacement.

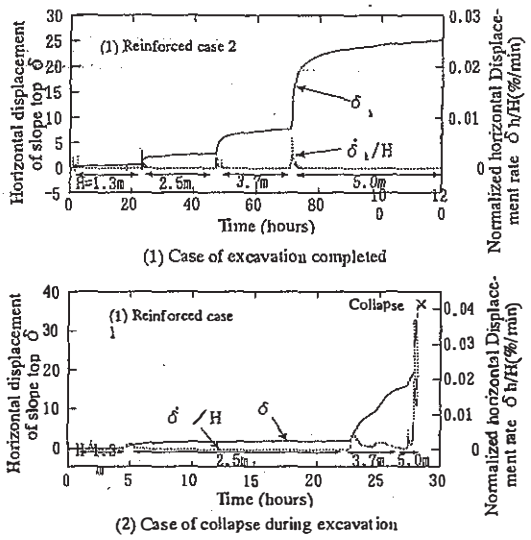

Figure 12. Relationship between horizontal displacement of slope top/normalized horizontal displacement and elapsed time.

3.2 Long-term stability of ground reinforced by the soil nailing method

Since the soil nailing method uses steel reinforcement, it is necessary to grasp the long-term durability against corrosion. In reinforced ground sites completed before 7 to 15 years ago, corrosion of reinforcing bars was studied by over-coring and material tests.[11] The nine slopes in Districts A to I investigated are shown in Table 4, with the number of years elapsed since the completion and geology.

In the study of corrosion, if the reinforcement top was covered with shotcrete, the tops of three reinforcing bars per slope were exposed by chipping off to be visually checked for corrosion. For this purpose, three rods for each of seven slopes A to G were sampled by over-coring 116 mm in outer diameter. The corrosion product on the sampled reinforcing bars was removed, and the corrosion area rate and pitting depth were measured. The corrosion area rate is the rate determined for each 10 cm portion in the longitudinal direction of reinforcing bar. The same reinforcing bars were also subjected to the tensile test.

The results of soil and water analysis revealed the fact that subject slopes were not in a severe corrosive environment.

Figure 13 shows the distribution of corrosion area rate of one typical reinforcing bar of each district. For District C, there was no corrosion. In the case of the reinforcing bars of Districts A, B, D, and E, corrosion was found in the portion not deeper than 30

Table4. Overview of the investigation sites *galvanized

Investigation site	Years after completion	Specification of reinforcement			Geology
		Kind, material	Length (m)	Drilled diameter (mm)	
A	10	D25, SD345	1.2	40	Mesozoic slightly weathered sandstone
B	8	D19, SD295	3.0	46	Palaeozoic slightly weathered tuff
C	9	D29, SD295	8.0	66	Talus cone deposit
D	9	D22, SD295	2.4	66	Palaeozoic weathered sandstone
E	15	D25, SD295	2.0	42	Palaezoic sandstone, crystalline schist
F	9	D32, SD295	2.0	46	Neogene mudstone, sandstone
G	7	D25, SD295	5.0*	40	Kanto loam
H	8	D25	4.0*	46	Neogene andesite, tuff
I	9	D25	4.0	66	Middle palaezoic sandstone, mudstone

cm from the surface. The corrosion of such depth was found with almost the half of the all bars. Pitting corrosion was also found in these bars. In the case of the reinforcing bars of Districts A, F and G, corrosion appeared in the portion deeper than 50 cm (though little for District G). In contrast, for Districts B, C and D where the grout covering thickness was 10 mm or more, there was no corrosion in deep levels.

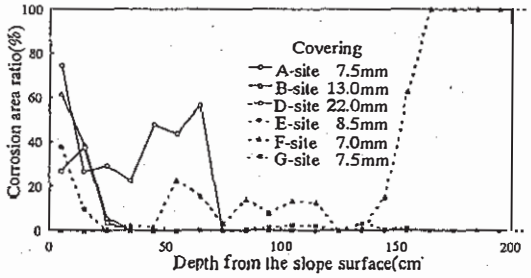

Figure13. Corrosion area ratio reinforcement in the depth direction.

Figure 14 is a schematic diagram of the presumed cause of corrosion. The corrosion in the portion not deeper than 30 cm from the surface may be caused by the insufficient filling of grout at the borehole mouth, due to infiltration of the grout into the ground at the time of injection. The corrosion in the deeper portion can be attributable to the unsatisfactory distribution of grout, due to the insufficient grout covering thickness. In the case of the galvanized reinforcement of District G, the corrosion is not significant either in the shallow or deep portion, though the grout covering is 10 mm or less thick. This proves the effectiveness of the galvanizing for preventing corrosion.

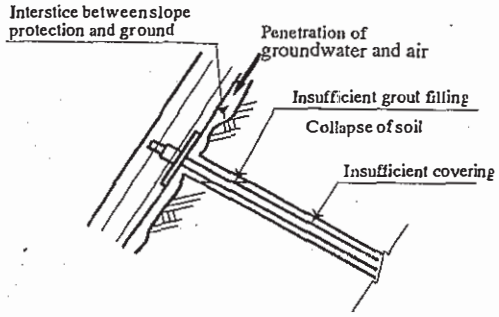

Figure14. Presumed cause of corrosion of reinforcement.

4 OVERVIEW OF THE DESIGN AND WORK PROCESS OF THE SOIL NAILING METHOD[10)]

This chapter discusses the design concept, safety management and corrosion requirements based on the results in 3.1, 3.2, summarizing the soil nailing method established in 1998.

(1) Stability calculation

In the applications of (1), (2) and (3) of Figure 15, the calculation uses the circular slip ultimate equilibrium equation based on the overall safety factor, the concept of which is shown in Figure 16.

Considering the fact that even in the ultimate equilibrium state, the tensile force does not reach the maximum allowable value in every reinforcing bar, the allowable tensile force is decreased by the reduction coefficient λ.

$$Fs = \frac{\Sigma(W \cdot \cos\alpha \cdot \tan\phi + c \cdot l) + \Sigma T_w(\cos\beta + \sin\beta \cdot \tan\phi)}{\Sigma W \cdot \sin\alpha} \quad (1)$$

$$T_{aw} = \lambda \cdot T_{pa} \quad (2)$$

where W = slipping earth mass (kN/m)

α = angle of slip surface to horizontal (degrees)

ϕ = internal friction angle on the slip surface (degrees)
c = cohesion on the slip surface (kN/m^2)
l = slip surface length of slice (m)
β = angle of reinforcement to slip surface (degrees)
Tpa = tensile strength of reinforcement evaluated by resistance performance (kN/bar)
Tav = tensile force induced in reinforcement (kN/bar)
λ = reduction coefficient (=0.7)

For designing total stability, the tensile strength T_{pa} of reinforcement must be determined, which is the smallest value among the following as indicated by Eq. 3, that is, pulling resistance T_{1pa} from the moving earth mass, pulling resistance T_{2pa} from the stationary ground, and the allowable tensile force of reinforcement T_{sa}. (Fig. 17)

$$T_{pa} = \min [T_{1pa}, T_{2pa}, T_{sa}] \quad (3)$$

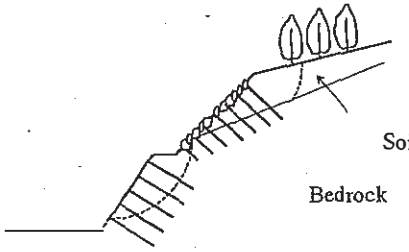

(1) Application to prevent middle-scale (collapse)

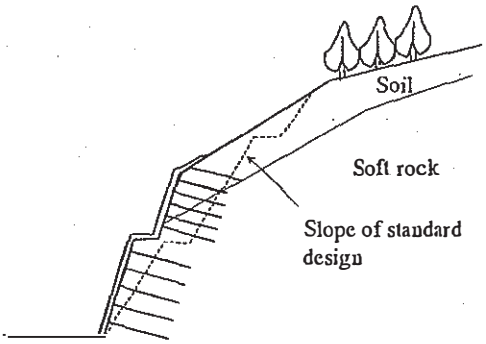

(2) Application to steep cuts

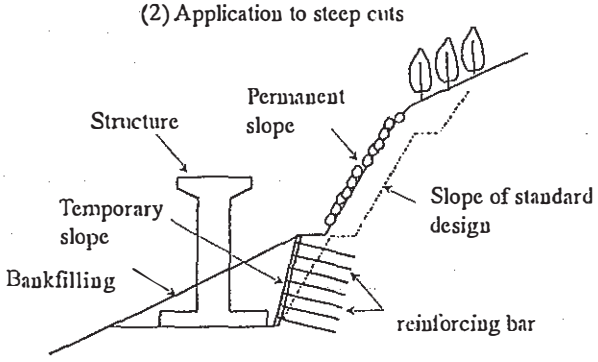

(3) Application as a temporary work to structure excavation

Figure15. Application of the soil nailing in Japan.

Through study of the recorded fracture patterns of nailed earth slope, we have found cases which may be due to push-out of moving earth mass. It is frequently induced by insufficient T_{1pa}. When a slope protection is provided, calculation of T_{1pa} solely based on the anchoring length leads to over-specification. In general, when a slope protection equivalent or superior to shotcrete slope crib is provided, T_{1pa} in Eq. 3 may be ignored. Without such a protection, T_{1pa} is determined, taking into full account the effect of slope protection work.

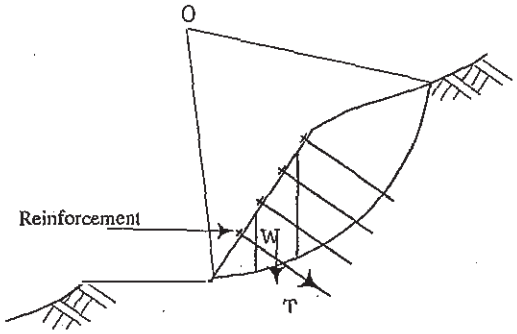

Figure 16. Calculation of stability by circular slip method.

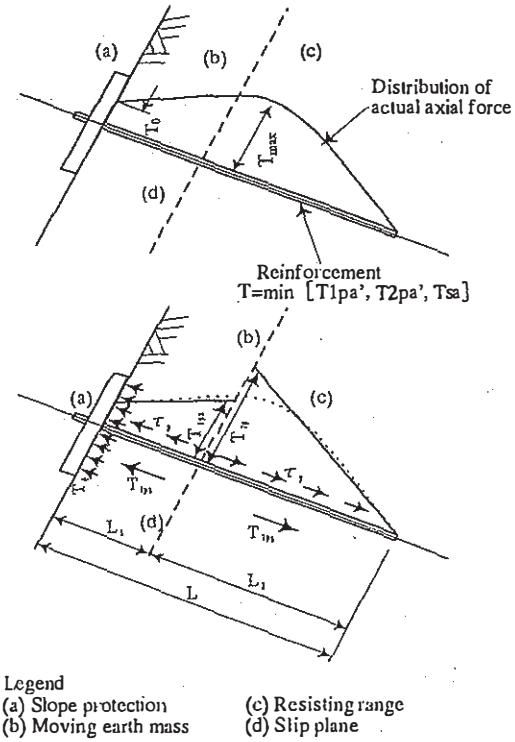

Figure17. Evaluation of tensile strength of the reinforcement.

(2) Anticorrosion method

On the basis of investigation results of the long-term stability discussed in 3.2, Designing and Construction Procedure for Soil Nailing provides the following requirements. When the soil nailing method is

used for a permanent work in an ordinary environment, galvanizing of the reinforcement is specified as a standard practice. In the design, a corrosion margin of 1 mm shall be considered in addition to the nominal diameter of the reinforcing bar. In addition, for ensuring a covering of 10 mm on each side, a spacer shall be placed at intervals of not more than 2.5 mm.

(3) Safety management standard for work

Any method of management will be costly that requires measurements to be made by many instruments such as borehole inclinometer and axial force meter of reinforcement. Such management does not take advantage of the economical efficiency of the soil nailing method. So, simple safety management is considered as a usual practice, solely based on monitoring of displacement at the slope top. Referring to the experimental work, full-scale test and case analysis discussed in 3.1, the criteria for safety management illustrated in Figure 18 were set up. The limit value of normalized horizontal displacement δ_h/H obtained by the full-scale test and case analysis was specified as "stop level", the value less than one half of it as "normal level", and the value between "stop level" and "normal level" as "warning level". At the warning level, either stop level or normal level is to be selected according to the e xtent of the strain rate convergence.

Since the soil nailing method allows deformations, strict management of displacement is essential when an important structure exists on the excavated slope. The work method with such an information-based management was proposed separately.

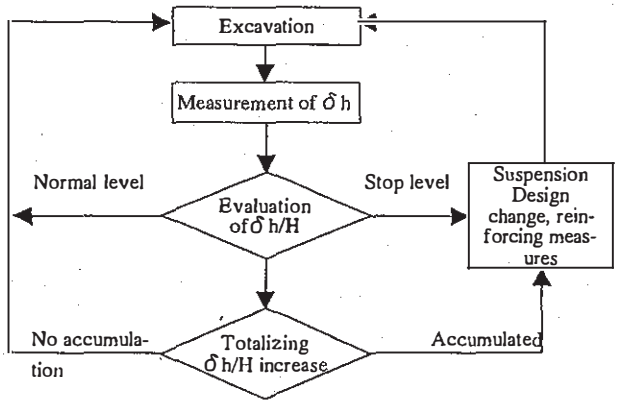

(in : %)

	Normal level	Warning level	Stop level
Soil	$\delta_h/H \leqq 0.20$	$0.20 < \delta_h/H \leqq 0.40$	$0.40 < \delta_h/H$
Soft rock	$\delta_h/H \leqq 0.15$	$0.15 < \delta_h/H \leqq 0.30$	$0.30 < \delta_h/H$
Hard rock	$\delta_h/H \leqq 0.10$	$0.10 < \delta_h/H \leqq 0.20$	$0.20 < \delta_h/H$

Figure 18. Stability mauagement flow during construction.

5 RECENT STUDY

This chapter describes the new boring technique and earth retaining work being developed by JH for the soil nailing method, and the centrifugal model test carried out for the purpose of evaluating the seismic performance of the soil nailing method.

5.1 *Development of new boring technique*

(1) · Background

When collapse of the drilled wall is anticipated in the soil nailing for constructing a permanent slope, casing drilling is usually implemented using a rotary or rotary percussion drill. However, this method costs about twice as much as the ordinary rod drilling with a crawler drill. Figure 19 shows the statistics of drilling machines used in expressway construction projects by the soil nailing method in 1999. Costly work with rotary and rotary percussion dril l-ing machines accounts for about 30 %.

The soil nailing method will be used more frequently in narrow sites such as structure excavation on a steep slope. There has been therefore demand for cost reduction by development of new drilling methods and new machines.

We will introduce below the characteristics of the newly developed drilling method (air grout drilling) and drilling machine (dual mode drill), and drilling test in actual construction sites and experimental work results.

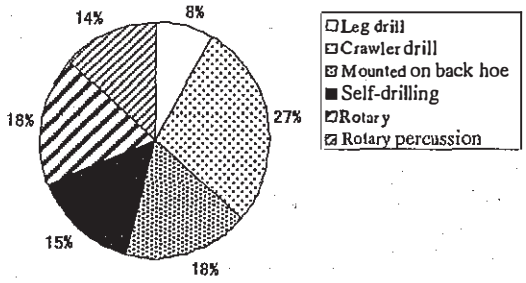

Figure 19. Breakdown of drilling machines.

(2) Characteristics of the new drilling technique (air grout drilling)

This technique continuously drills holes, while spraying cement milk with compressed air through the drill rod bit. It has enabled 10 m deep drilling even in the ground prone to collapsing when drilled. Figure 20 is the section of the reinforcing bar cut in half. This bar was dug up after it had been driven into an embankment by the soil nailing method, which presumed a ground prone to collapse when drilled.

The cement milk sprayed over the drilled wall with compressed air penetrates into the ground out-

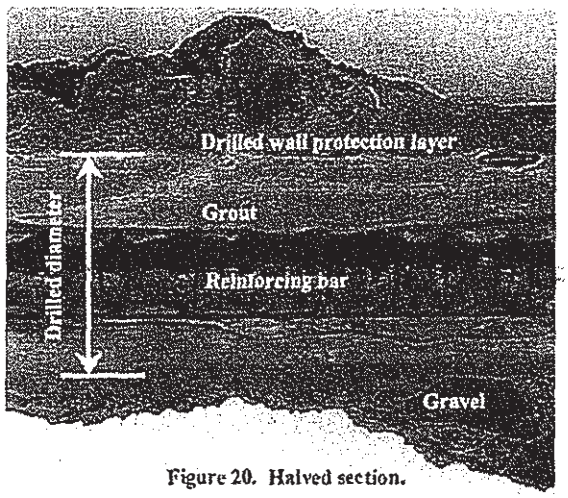

Figure 20. Halved section.

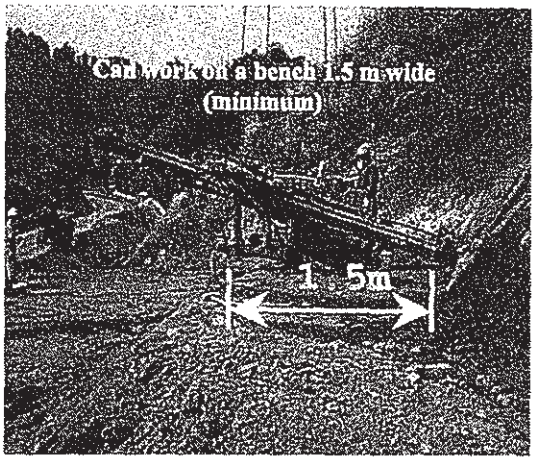

Figure 21. View of the machine working on the skid.

side the drilled holes. This prevents collapse of gravels, etc.

(3) Development of drilling machines

The dual mode drill has been developed for the air grout drilling method which can be used in sites with limited space for working.

The dual mode drill has the following features.

[1] It can be used for both air grout drilling and air drilling (drilling only with drilling bit and compressed air). The operator can switch between these methods, taking into account the geology of the site.

[2] The main drill unit and the crawler undercarriage frame can be easily mounted and dismounted. In a narrow elevated site, the drill can be mounted on the skid base, so it can work suspended by a crane. This ensures efficiency since only one drill is needed. The skid type can work in a space as narrow as 1.5 m. (Figure 21)

[3] A swinging base frame is provided on the crawler type undercarriage. On the base frame, a boom with a large rising angle is provided. This feature allows work over the whole range of the slope, even in a narrow bench where it in impossible to change the direction of the crawler drill and only movement parallel to the slope is possible, without turning the drill unit. (Fig. 22)

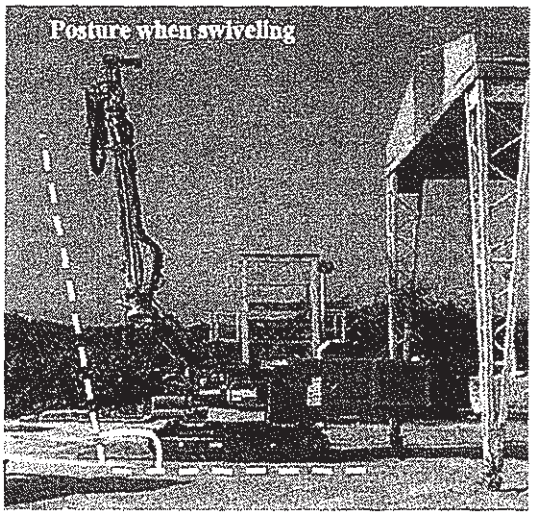

Figure 22. Posture when swiveling.

(4) Drilling test in a ground prone to collapse when drilled

1) Overview

To verify the applicability of the air grout drilling method, a field drilling test was conducted. Table 5 summarizes the specifications of the drilling test.

Table 5. Specification of the test.

Drilling type	Drilling length (m)	Re-bar length (m)	Re-bar diameter	No. of holes	Drilling diameter (mm)
Self-drilling	10.0	10.2	ϕ28.5	1	ϕ50
Air grout drilling	10.0	10.2	D25	4	ϕ65
5 m air grout + 5 m air drilling	10.0	10.2	D25	2	ϕ65
Air drilling	10.0	10.2	D25	2	ϕ65

Three methods were used to compare work performance. These methods were self-drilling method (cutting bit is mounted on the reinforcing bar, and it is left in the drilled hole), air grout drilling method, and switching to air drilling in the course of air grout drilling. The grout working performance was also checked. The switching method assumed a ground with hard lower layer, whose surface layer is prone to collapse when drilled. The geology of the test site is mainly composed of sedimentary rocks of Neogene Hamaishidake group Naka-kawachi formation, covered with Quaternary unconsolidated deposits.

2) Results of the drilling test

The drilling test results are shown in Figure 23. The drilling time was almost the same for the three methods, 20 to 30 minutes. But in the case of Drilling No.1, i.e., 5 m air grout drilling + 5 m air drilling, the drilling time was significantly longer. This is attributed to the existence of ground water in the air drilling at levels deeper than 5 m, which made it difficult to return the slime.

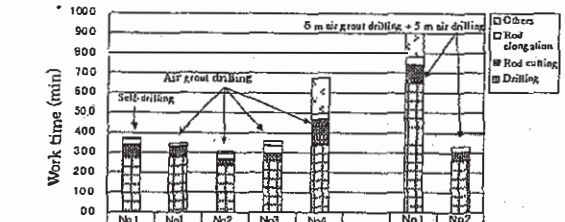

	No.1	No.1	No.2	No.3	No.4	No.1	No.2
Others	0.8		1.3	2.5	18.0	12.2	
Rod elongation	2.7	1.7	2.8	3.8	2.9	3.9	2.7
Rod cutting	6.3	5.0				8.8	4.3
Drilling	27.7	28.3	24.0	26.1	34.2	65.4	26.3

Figure23. Drilling time.

The grout working performance dug out was compared among the air drilling, air grout drilling and self-drilling. Both with the air grout drilling and air drilling, the grout is about 70 to 80 mm in diameter, and no hole bending was found. However, gravel was mixed in the grout with the air drilling.

With the self-drilling, the grout filling was insufficient in the vicinity of the hole mouth, and the reinforcing bar was partially exposed. (Fig. 24)

Since there is a fear of unsatisfactory grout filling with self-drilling, the Designing and Construction Procedure for Soil Nailing Method of the JH[10] allows its use only for temporary work. This drawback of the self-drilling was also demonstrated by our test.

(5) Experimental work in ground prone to collapse when drilled

In order to verity the continuous work performance of the air grout drilling, a test work was implemented in a construction site of expressway. The specifications of this work are shown in Table 6.

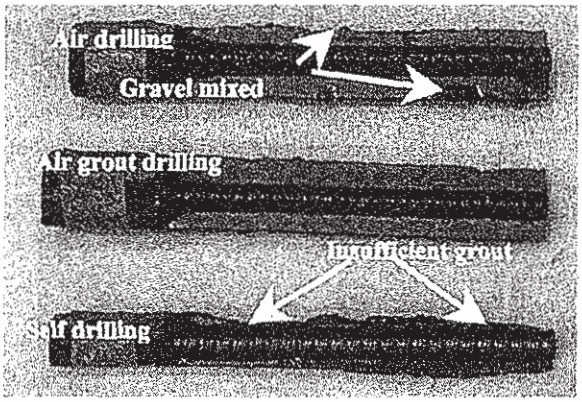

Figure 24. Dug out grout working performance.

Table 6. Specification of continuous work test.

Case	Ground	Drilling method	Drilling length (m)	Re-bar length (m)	Re-bar diameter	No. of holes	Drilling diameter (mm)	Remarks
1	Weathered rock	AIR GROUT drilling	2.9	3.0	D25	92	ϕ65	
2		Rotary percussion	2.9	3.0		272	ϕ90	

In the experimental work, the performance of the air grout drilling was compared with that of the rotary percussion method used in the same slope. The geology of the site was composed of alternate strata of heavily weathered sandstone and shale.

Figure 25 illustrates the comparison of average time of one work cycle between air drilling and rotary percussion used in the same slope. The average time of rotary percussion is 44 minutes, while that of the air grout drilling is 31 minutes, that is, about 30% shorter. This difference was chiefly due to the difference in drilling time. In the case of the rotary percussion, the casing is 1 m long, requiring that the tube be extracted. In contrast, the air grout drilling uses a 3 m rod, which eliminates the operation of connecting and extracting the tube.

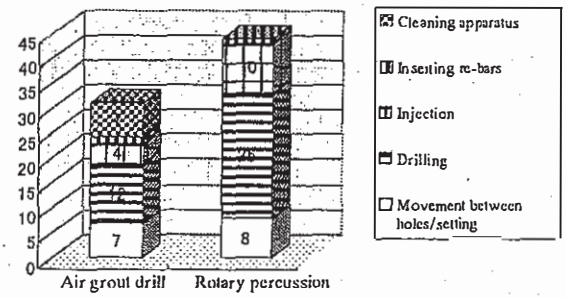

Figure25. Breakdown of work time.

(6) Prospect

We are intending to use the air grout drilling technique as a standard method for work in drilling in grounds prone to collapse.

5.2 *New structure excavation method using the soil nailing method*

(Angle cut cylinder earth retaining work)[18]

(1) Background

When excavating for building a structure such as pier on a steep slope in a mountainous district, either usual slope cut or ground anchoring is generally employed to cut and retain earth. The cutting on a steep slope tends to be over a large area, significantly altering the natural environment and producing a large amount of excavated soil. On the other hand, retaining the earth also uses ground anchoring, with sufficiently long piles driven in the steep slope. This requires installation of work stages, resulting in a long work period and an enormous work cost. JH proposed an excavation technique as illustrated in Figure 26 for building structures, mainly based upon the work method (angle cut cylinder earth retaining). This technique ensures a high stability, hardly disturbing the in-situ equilibrium of earth pressures and limiting the alteration of the natural environment. This chapter discusses the overview of the new technique and the behavior of each structural component in the test work.

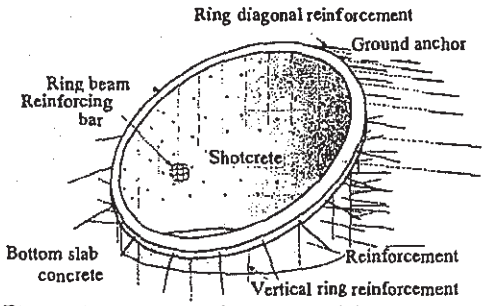

Figure26. Angle cylinder earth retaining.

(2) Overview of the structural members used in the angle cut cylinder earth retaining

The structural members used in this technique have the following functions.

[1] Ring beam

A high rigid ring beam is formed on the ground surface before excavation. This limits the displacement (in the forward direction) of the upper sprayed portion during excavation. Consequently, the shear strain generating in the ground becomes smaller, not significantly degrading the ground stability. When the ground anchors are placed, the ring is also used as panel to absorb pressure.

[2] Ring diagonal reinforcement

This component resists the sliding of the ring beam. The reinforcing members are installed in the radial pattern, aiming at the pre-installed reinforcement effect.

[3] Ground anchor

This component limits the displacement of the whole of the structure.

[4] Shotcrete

Shotcrete is placed for resisting the earth pressures and protecting the ground.

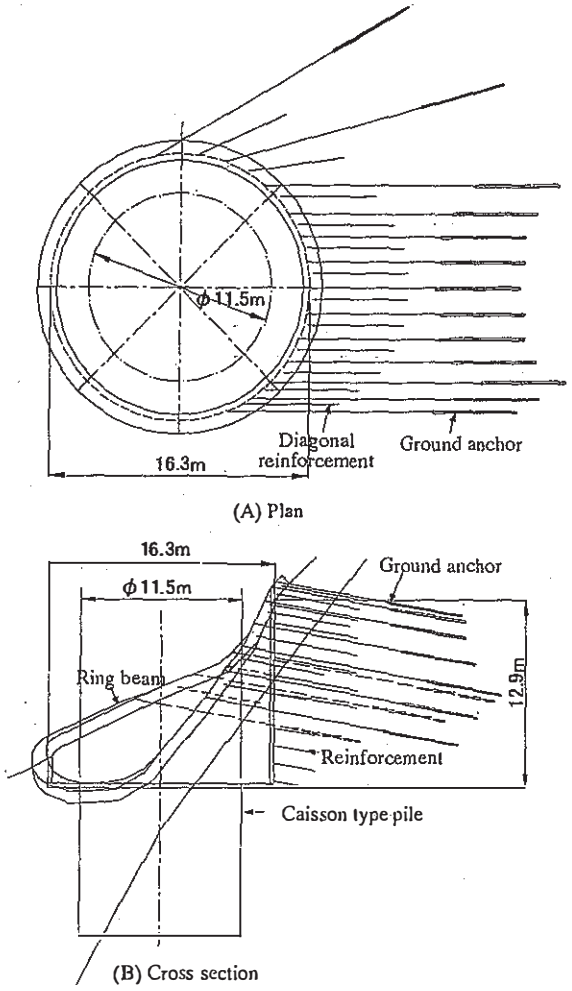

Figure27. Plan and cross section of the angle exc. cylinder earth retaining.

[5] Reinforcement

Integrated in the ground, the reinforcement increases the ground stability against stresses in

the ground, limiting the deformation. As a result, it reduces earth pressures acting on the shotcrete. In addition, it temporarily supports the dead weight of the ring beam and shotcrete during excavation work. When a slip surface is produced in the ground, it resists the slip force in the region deeper than the slip surface.

(3) Behavior of the angle cut cylinder earth retaining method in the experimental work

Figure 27 depicts the outline plan and section of the experimental work. The geology of the experimental work site is mainly composed of alternate strata of heavily weathered sandstone and shale.

Figure 28 illustrates the surface displacements determined by an electro-optical survey. In general, the ring beam displaces toward the lowest topographical level (lower left viewed from the mountain side). This can be explained as follows. The reinforcing bars that prevent the slide of the ring beam were placed in the range of about 120 degrees around the maximum height of excavation on the mountain side, but the displacement occurred in the direction oblique to the reinforcing bars. As a consequence, the reinforcing bars failed to provide a sufficient resistance against slide.

Figure 29 shows the ground displacements determined by insertion type borehole inclinometers installed in the locations indicated in the same figure. In each of the three locations, the ground displaced in such a way that it fell down toward the excavation surface. During excavation for caisson type pile foundation, the displacement tended to increase. Although location ② (excavation height H = 5.9 m) is the lowest among the three locations, the normalized slope top displacement δ_h/H (ratio of horizontal displacement to excavation height in percentage) was 0.26 % at maximum, which was the largest among the three locations. This is caused by the geology of the area. The ground at location (2) from the cutting start level to the excavation bottom is entirely covered with heavily weathered conglomerate, and the measurement data show a settlement of 22.7 mm at this location, which is double the settlement at the other two locations, around 10 mm. The maximum horizontal displacement took place below the slope top. This verifies the effect of the ring beam limiting the displacement at the slope top.

Figure 30 illustrates the axial force in the reinforcement and stress in the reinforcing bars and concrete of the wall. The maximum axial force generated in the reinforcement was about 70 kN, which is 60 % of the designed axial force of 118 kN, in location ③ of the wall reinforced by the "layer-by-layer placement" method. According to the records of previous projects that excavated steep slopes, the actual axial force generated in the reinforcement is in most cases about 30% of the allowable axial force.

The large axial force in location (3) was induced by the vertical excavation, about 13 m high at maximum, where larger displacements than usual occurred. The axial force was large in the upper portion of excavation, and tended to decrease in deeper excavation levels. This result approximately agrees with the ground displacement distribution. On the other hand, the maximum compressive stress in concrete was 0.1N/mm^2 both in vertical and transversal directions, and the maximum tensile stress in the reinforcing bars was 1 N/mm^2. These measured values are very small in comparison with the axial force in the reinforcement.

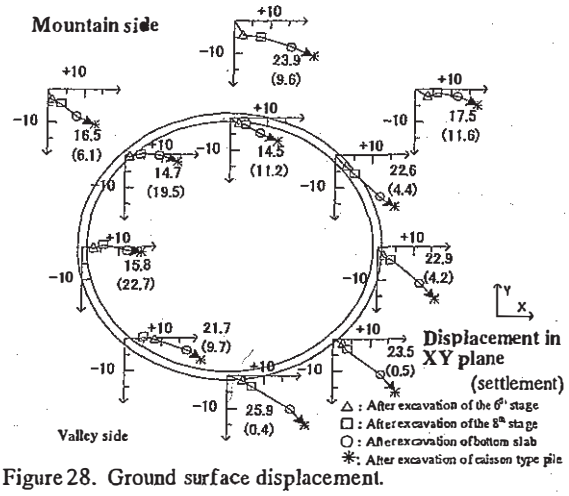

Figure 28. Ground surface displacement.

The behavior measured in the field of the angle cut cylinder excavation is summarized as follows. [1] The slope top horizontal displacement γ max does not necessarily occur at the highest excavation position. The displacement tends to increase, also during excavation for pier foundation. Work Safety Management requires measurement be made on the lateral sides, and during pier foundation excavation too. [2] The magnitude of the displacement occurring in the weathered geology is about the same as it is in talus. [3] The section of the ring beam on the valley side may vary with the topography of the site. Therefore, the reinforcing bars for limiting the sliding driven in the direction of maximum excavation depth on the mountain side, are not effective in some cases. [4] The stresses in the reinforcing bars and concrete in the wall are very small, whereas the axial forces in the reinforcement are large. This proves that the reinforcement as a whole works to resist earth pressures, limiting the ground deformation. In conclusion, the section design can be based on the tensile force of the reinforcement.

(4) Plans for future study

The author will further study the design method of each structural component, referring to the experi-

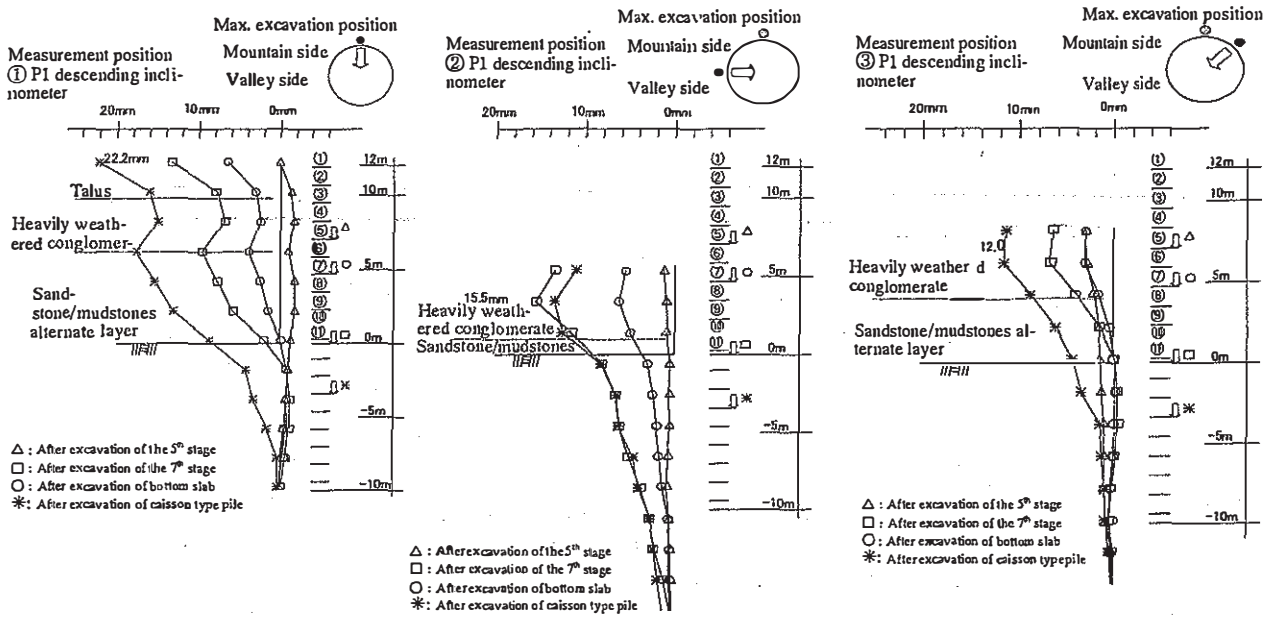

Figure 29. Ground displacement.

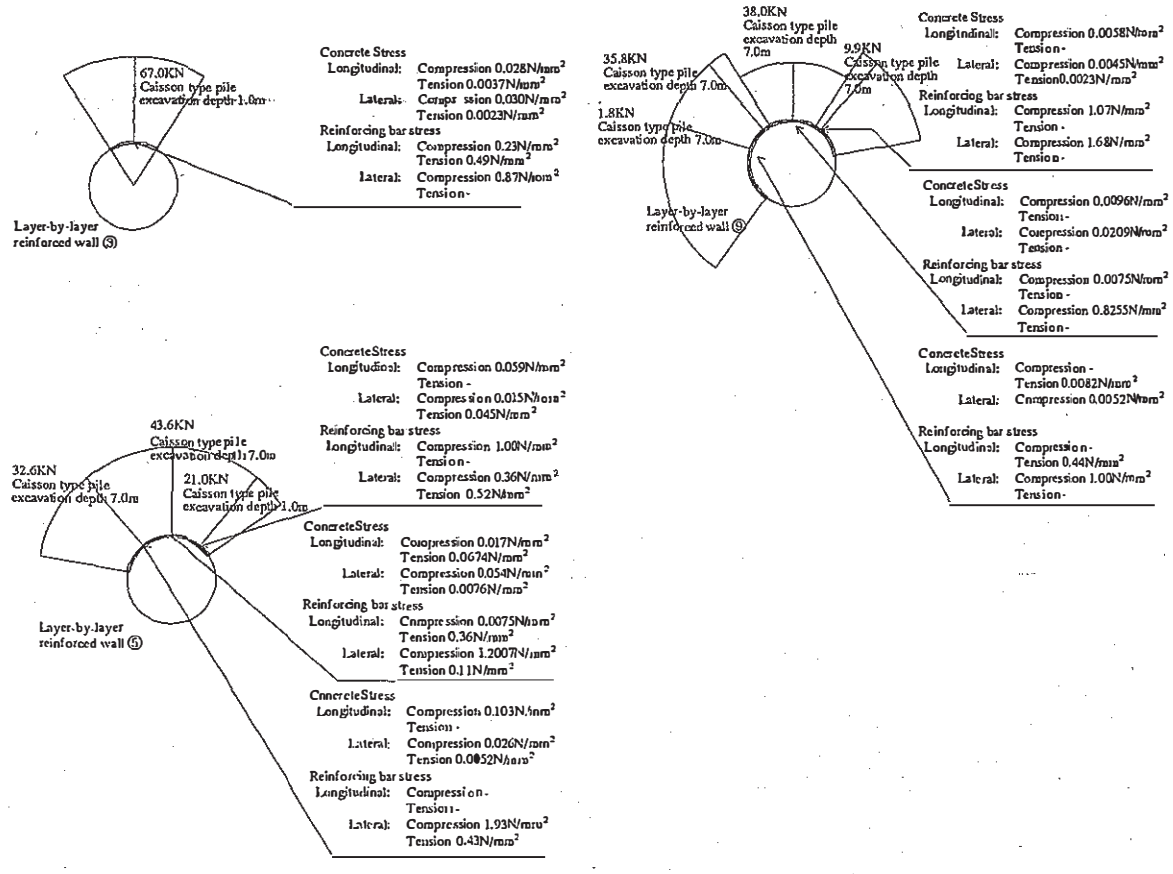

Figure 30. Axial force in reinforcement, stress in wall.

mental work results. Measurement date of structural components will be gathered and analyzed through additional experiments. In addition, the author will analyze the behavior in the ult imate stage of the ring beam, reinforcement and shotcrete, and ultimate fracture mode through fracture tests using models.

5.3 *Seismic performance of the soil nailing method (Centrifugal model test)* [19]

(1) Background

The seismic design is not usually implemented for cut slopes in Japan. But, the slope, which was improved by the soil nailing method, may be superior in seismic performance.

This chapter discusses the pull-out test of the reinforcement and centrifugal vibration test with a model slope conducted for the purpose of evalua ting the seismic performance of the soil nailing method.

(2) Materials for the test

In the centrifugal model test and pull-out test, DL clay was used as ground material. The water content of this clay was 20% and unit weight γ_t was 14 kN/m^3. The physical properties of the DL clay are shown in Table 7. The internal friction angel $\phi$was calculated from the consolidated drained test result, and the cohesion from the collapse test of a non-reinforced cut slope. The test employed guitar strings 0.58 mm in diameter (coiled string) for the reinforcing material, the diameter and shape of which are proportionally similar to the actual reinforcing material. Silicone adhesive and gypsum were used as injecting material, selected because of their fluidity and pull-out resistance.

Table 7. Physical properties of DL clay.

Soil particle density	2.675t/m^3
D_{50}	0.024mm
Max. void ratio	1.675
Min. void ratio	0.695
Internal friction angle	40.5°
Cohesion	9.2kPa

(3) Centrifugal model test of the soil nailing method

The test was conducted in a 50*g* centrifugal force field, with 100Hz sinusoidal wave inputted 4 times as a seismic wave as shown in Table 8. The model cut slope had a gradient of 1 : 0.3 and was 140 mm high (7.0 m, converted to full scale). The shape of the model ground of the centrifugal model test and sensor positions are shown in Figure 31. The reinforcement mode for each case is shown in Table forcement mode for each case is shown in Table 9. The reinforcing bars were placed at intervals of 30 mm (1.5 m, converted to full scale) in every case. For slope lining, OHP transparency sheets were applied over the slope with adhesive, which can prevent local collapse and has a small strength. (All the results presented here are the values converted to full scale)

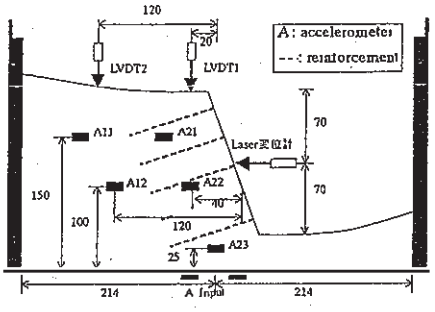

(in mm)

Figure31 Shape of soil nailing model and sensor position.

Table 8. Vibration conditions.

	Max. acceleration (g)	Wave number
Step1	6	20
Step2	12	20
Step3	15	20
Step4	15	40

Table 9. Reinforcement mode of the cases.

	Injection material	Drilling dia. (mm)	Placement length (mm)	Slope lining
CASE3	Non-reinforcement	—	—	Not provided
CASE4	Adhesive	2	80	Not provided
CASE5	Adhesive	2	80	Provided
CASE6	Gypsum	7	80	Provided
CASE7	Gypsum	7	40	Provided

Figure 32 depicts the displacement vectors in Step 2 of Cases 4 and 5. In Case 3 (without reinforcement) the ground is unstable (limit height 6.3 m). Reinforcement driven into the face significantly improved the seismic performance. However, a slip line occurred in the reinforced zone, which indicates poor internal stability. Through comparison of the position of slip line between Cases 4 and 5, we know that, without the slope lining, the slip line passes at a level much higher than the slope foot. This result verifies the effect of the lining. However, no significant difference was found in the relationship between settlement of the slope top and magnitude of the input seismic wave. This is caused by the slope lining applied in our test which had a small rigidity and thus did not noticeably contribute to restraining deformation, and made no significant difference in the fracture mode.

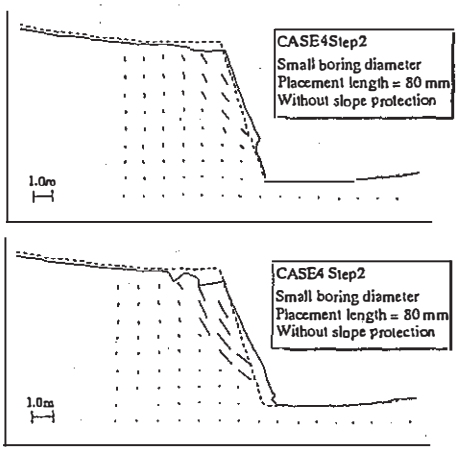

Figure 32. Displacement vector diagram of Cases 4 and 5 (Step 2).

Figure 33 shows the change of slope top settlement along with time in Steps 1 and 2 of Cases 5 and 6. In Case 5, a large settlement took place in Step 1, whereas in Case 6, though the settlement occurred when vibration was applied but its magnitude was small, and no collapse was observed. From this result, we can conclude that with larger drilling diameters, the residual displacement of the cut earth can be restrained to a small magnitude.

(4) Friction characteristics of the reinforcement and ductility of the nailed cut slope

As a general rule, the effect of reinforcement is exhibited when a relative slip is generated between the reinforcement and surrounding earth mass. Cut earth without reinforcement is easily fractured, whereas nailed cut earth shows a larger displacement till it fails. In order to investigate the relationship between seismic scale and ductility of the reinforced region, the author worked out a formula to express the relationship between seismic scale and the deformation of the cut earth applying the Arias Intensity (Ia) by Arias and Kayen & Mitchel.

The seismic scale (energy) till Step n is given by

$$\sum_{i}^{n} I_a(T_i) = \sum_{i}^{n} \frac{\pi}{2g} \int_0^{T_i} a^2(t)dt$$

where

g = gravitational acceleration (9.8 m/sec^2), T_1 = vibration time in Step I, a = input acceleration.

In Figure 34, the seismic scale is plotted against the abscissa axis, and the accumulated settlement till collapse against the ordinate axis. In Cases 4 and 5 with a smaller drilling diameter, abrupt collapse took place when the slope top settlement exceeded 100 mm. This corresponds to about 2 mm settlement on the model scale, which is approximately equal to the pull-out amount when the peak strength is reached in the pull-out test. We can therefore conclude that, when the accumulated displacement exceeded 10 mm during vibration, the pull-out shear stress in the reinforcement skin reached its peak value and led to an abrupt settlement. In conclusion, if the friction characteristics of the reinforcement and ground are known from the pull-out test of the reinforcement, it is possible with some accuracy to predict the deformation performance of the nailed cut slope.

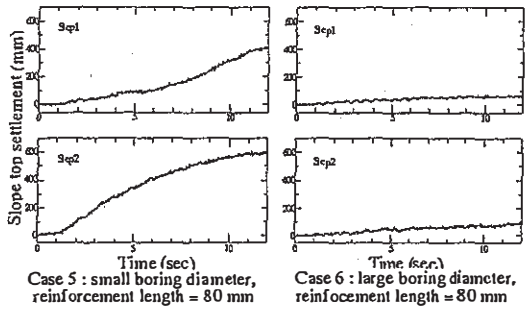

Figure 33. Displacement vector diagram of Cases 5 and 6 (Step 2).

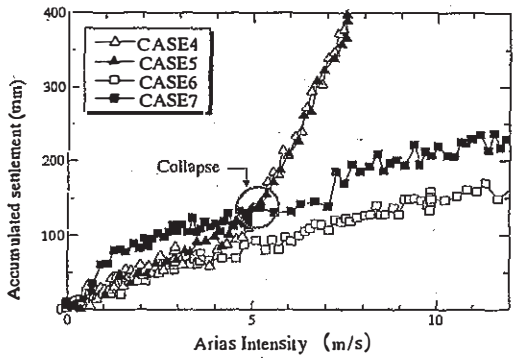

Figure 34. Accumulated settlement vs. input seismic energy

(5) Summary of the test results

The results of the test on the seismic performance of the soil nailing method are summarized as follows.

[1] The method improves the deformation performance of cut earth, offering higher ductility.

[2] With longer reinforcement and larger drilling diameter, the deformation performance is improved drastically.

[3] If the friction characteristic between the reinforcement and ground can be appropriately evaluated, it is possible to predict the deformation of the nailed cut slope with a certain accuracy under seismic acceleration.

6 CONCLUSIONS

The soil nailing method is one of the most effective measures to meet the diversified needs in road construction sites in mountainous Japan, such as collapse prevention and steeper structure excavation. However, problems remain to be solved as discussed in the introduction. We expect that the potential of this method will be more fully exhibited in work sites through further investigations in various research institutes on such problems.

REFERENCES

1) Tatsuoka,F., Kondo,K., Miki,G., Ikuhara.O., Hamada,E., Sato,T. 1983. Fundamental study on the reinforcement of sand with tensile reinforcement. Soil and Foundation Vol.31, No.9 SerNo.308, pp.11-19
2) Hayashi,H., Ochiai,H., Sakai,A., Tayama,S. 1986. Effect of head plate in the reinforced earth mechanism of slope with reinforcing bars. Proceedings of Japan Society of Civil Engineers No.367/VI-4, pp.62-70
3) Nishimura,K., Yamamoto,M. 1987. Stabilization of cut slope by relatively short rock bolts, Proceedings of Japan Society of Civil Engineers, No.388/III-8, pp.217-226
4) Okuzono,S., Okuhara,T., Nagao,A. 1985. Field load test of slope improved with reinforcing bar. Report of Japan Highway Public Corporation Research Institute Vol.22, pp.35-44
5) Okuhara,T., 1986. Load test and application to work sites of the cut slope reinforcing method. Civil Engineering Vol.41 No.10, pp.60-67
6) Kitamura,T., Nagao,A. 1988. Experimental study on the reinforcing effect of the model sandy slope improved with reinforcing bars subject to vertical load, Proceedings of Japan Society of Civil Engineers No.391/ VI -8 , pp.188–195
7) Mori,S., Asahi,M. 1986. Experimental work of cut slope improved with reinforcing bars. Civil Engineering , Vol.41, No.10, pp.68-72
8) Japan Highway Public Corporation 1987. Designing and construction data of soil nailing method
9) Study committee of reinforced slope method, Committee report, Proceedings of symposium on the Reinforced slope Method
10) Japan Highway Public Corporation. October 1998. Designing and Construction Procedure for Soil Nailing Method
11) Scientific Committee of the French National Project Clouterre. August 1993. "Recommendations Clouterre 1991 (English Translation : Soil Nailing Recommendations-1991)"
12) Nagayoshi,T., Tayama,S., Ogata,K., & Tada,M., 1999. Full-scale model test on deformation of reinforced steep slopes. Proceedings of the international symposium on slope stability engineering
13) Study committee of reinforced slope method 1996. Committee report, Proceedings of symposium on the reinforced slope Method
14) Hori et al. Construction cases of earthwork improved with reinforcing bars. Japan Society of Civil Engineers, 46th Annual meeting for reading research papers
15) Suami et al. Effect of slope protection by earthwork improved with reinforcing bars (Part 2). 27th geotechnical meeting for reading research papers
16) Ito et al. Cases of earth retaining work with wall by earth improvement with reinforcing bars, geotechnical meeting for reading research papers
17) Sakurai 1988. Design and Construction Manual of NATM in urban areas. Kansai branch of Japan Society of Civil Engineers. Committee for application of NATM to tunneling in urban areas
18) Sato,A., Tayama,S., Ogata,K., Takemoto,M., Tanaka,U. Behavior of Angle Cut Cylinder Excavation by Cut Reinforced Earthwork Method
International Symposium Earth Reinforcement IS Kyushu 2001
19) Kusakabe,O., Takahashi,A., Tayama,S., Takemoto,M. Centrifugal model tests on seismic stability of reinforced cutting slope
The Japanese Geotechnical Society 2000 Vol.35 2/2 p2197-2198
20) R.E.Kayen & J.K.Mitchell 1997. Assessment of liquefaction potential during earthquakes by Arias intensity. J.Geotech & Geoenvir. Engrg., ASCE, 123 (12) , pp1162-1174,